J Ginseng Res 45 (2021) 156–162

Contents lists available at ScienceDirect

Journal of Ginseng Research

journal homepage: http://www.ginsengres.org

Research Article

# Identification of N,N′,N″-triacetylfusarinine C as a key metabolite for root rot disease virulence in American ginseng

Jacob P. Walsh [1,2], Natasha DesRochers [1,2], Justin B. Renaud [1], Keith A. Seifert [4], Ken K.-C. Yeung [2,3], Mark W. Sumarah [1,2,*]

[1] London Research and Development Center, Agriculture and Agri-Food Canada, London, ON, N5V 4T3, Canada
[2] Department of Chemistry, University of Western Ontario, London, ON, N6A 5B7, Canada
[3] Department of Biochemistry, University of Western Ontario, London, ON, N6A 5C1, Canada
[4] Ottawa Research and Development Centre, Agriculture and Agri-Food Canada, 960 Carling Ave., Ottawa, ON, K1A 0C6, Canada

ARTICLE INFO

*Article history:*
Received 12 February 2019
Received in Revised form
30 May 2019
Accepted 22 August 2019
Available online 13 September 2019

*Keywords:*
Siderophore
Root rot
*Panax quinquefolius*
*Ilyonectria mors-panacis*

ABSTRACT

*Background:* It is estimated that 20–30% of ginseng crops in Canada are lost to root rot each harvest. This disease is commonly caused by fungal infection with *Ilyonectria*, previously known as *Cylindrocarpon*. Previous reports have linked the virulence of fungal disease to the production of siderophores, a class of small-molecule iron chelators. However, these siderophores have not been identified in *Ilyonectria*.
*Methods:* High-resolution LC–MS/MS was used to screen *Ilyonectria* and *Cylindrocarpon* strain extracts for secondary metabolite production. These strains were also tested for their ability to cause root rot in American ginseng and categorized as virulent or avirulent. The differences in detected metabolites between the virulent and avirulent strains were compared with a focus on siderophores.
*Results:* For the first time, a siderophore N,N′,N″-triacetylfusarinine C (TAFC) has been identified in *Ilyonectria*, and it appears to be linked to disease virulence. Siderophore production was suppressed as the concentration of iron increased, which is in agreement with previous reports.
*Conclusion:* The identification of the siderophore produced by *Ilyonectria* gives us further insight into the root rot disease that heavily affects ginseng crop yields. This research identifies a molecular pathway previously unknown for ginseng root rot and could lead to new disease treatment options.


## 1. Introduction

Ginseng has been used as a traditional medicine for hundreds of years [1]. The ginseng species *Panax quinquefolius* (American ginseng) is a valuable cash crop in Canada and the United States [2]. Canada is one of the largest exporters of ginseng in the world, generating approximately 100 million dollars (USD) in revenue annually [3]. Despite its high value and popularity, the cultivation of this crop is challenging. Ginseng seeds take more than a year to germinate before they can be planted and 3–4 years to reach maturity before harvesting. The crop is at high risk of replant disease, where new ginseng cannot grow in fields where a ginseng crop has already been grown, an effect that may last for decades [4]. Several factors are believed to contribute to replant disease including an accumulation of phytotoxic compounds, changes in soil microbiomes, and persistent soilborne fungal diseases [4].

There are two general categories of fungal diseases affecting ginseng crops, foliar diseases and soilborne diseases. Foliar diseases take the form of blight or anthracnose, typically caused by fungal infections of species of *Alternaria* or *Botrytis* [5]. Foliar diseases are often managed by application of fungicides and are a seasonal issue. Soilborne fungal diseases are more difficult to manage and include root rot and rusty root, both of which may persist in fields for years. The fungal species *Cylindrocarpon destructans* was traditionally thought to be the main cause of ginseng root rot, but a recent taxonomic review reclassified it into several phylogenetically distinct *Ilyonectria* species [6]. Specifically, species most often responsible for root rot disease were identified as *Ilyonectria mors-panacis* [6,7]. *Ilyonectria* species infect roots of ginseng plants and either kill the plant, in the case of root rot, or lower its quality, in the case of rusty root [8]. Current methods of managing root rot are ineffective, and it

* Corresponding author. London Research and Development Center, Agriculture and Agri-Food Canada, London, ON, N5V 4T3, Canada.
*E-mail address:* mark.sumarah@canada.ca (M.W. Sumarah).

https://doi.org/10.1016/j.jgr.2019.08.008
p1226-8453 e2093-4947/$ – see front matter 

is estimated that between 20–30% of crop yield is lost to this disease annually [2].

*Ilyonectria* species may infect a wide range of hosts. In addition, both virulent and avirulent strains have been observed. Rahman and Punja [9,10] examined factors affecting ginseng root rot and related high iron concentration in soil to high disease virulence. They also proposed that increased virulence is associated with production of siderophores [10]. Siderophores are secondary metabolites produced by microorganisms to chelate iron found in the environment and effectively transport it into the cell [11,12]. Although siderophore production and its association with virulence was reported, the identity of the siderophore was not determined.

In this study, we used a semitargeted LC–MS approach to detect and identify the siderophore produced by *I. mors-panacis* and examined differences in siderophore production between virulent and avirulent strains. We also monitored the effects of $Fe^{3+}$ and ethylenediaminetetraacetic acid (EDTA) concentration in liquid media on siderophore production.

## 2. Materials and Methods

### 2.1. Fungal species and growth conditions

Fungal strains were obtained from the Canadian Collection of Fungal Cultures (DAOMC) and Dr Keith A. Seifert (Table 1). Strains that had previously been used in pathogenicity assays on *P. quinquefolius* were chosen. Strains that did not have direct assay data were chosen owing to their close relationship to the aforementioned strains, confirmed by their beta-tubulin sequences [7].

Cultures were grown on potato dextrose agar media [potato dextrose broth, 2.4% (*w/v*); Sigma-Aldrich, ON, CA, and agar, 2% (*w/v*); Fisher Scientific, NJ, USA] at 23°C until the culture diameter reached approximately 3 cm. The colony was excised from the agar plate and macerated using a Polytron blender (Brinkmann Instruments, Rexdale, Ontario, CA) in autoclaved distilled water. A 5% (*v/v*) aliquot of the macerated material was used to inoculate 25 Roux bottles, each containing 200 mL of potato dextrose broth [potato dextrose broth, 2.4% (*w/v*); Sigma-Aldrich] dissolved in distilled water. Cultures were incubated stationary for 20 days at 21°C.

### 2.2. Assessment of virulence against ginseng

A virulence assay was performed on two-year-old American ginseng roots, obtained from Ontario Ministry of Agriculture, Food and Rural Affairs, research plots located in Southwestern Ontario, Canada. Loose soil on the roots was rinsed off with distilled water, and roots were exposed to biocidal UV light for 10 minutes per side. Each strain was tested in quadruplicate. A 0.5-cm cross-incision (Fig. 1) was made into the root, and a 0.5-cm agar plug taken from the aforementioned growth plate was pinned in place over the incision. Inoculated roots were placed in sealed containers using wet paper towels and stored at 21°C. After 21 days, the ginseng was assessed for disease, and the lesion diameter was measured to determine disease virulence. Controls consisted of ginseng roots with an incision only.

**Table 1**
Species and strain information of fungal isolates studied and the host organism.

| Name | DAOMC | Host organism (common name) |
|---|---|---|
| *I. mors-panacis* | 251601 | *Panax quinquefolius* (American ginseng) |
| *I. mors-panacis* | 251604 | *Panax quinquefolius* (American ginseng) |
| *I. mors-panacis* | 251605 | *Panax quinquefolius* (American ginseng) |
| *I. rufa* | 251608 | *Pseudotsuga menziesii* (Douglas fir) |
| *I. rufa* | 251609 | *Picea glauca* (white spruce) |
| *C. obtusisporum* | — | *Picea mariana* (black spruce) |

*C. obtusisporum* (KAS 8150) is held in the laboratory collection of K.A.S. and is as of writing not recorded with the DAOMC. DAOMC, Canadian Collection of Fungal Cultures.

### 2.3. Extraction of metabolites

The mycelia of the cultures were separated from liquid media using Whatman #4 filter paper. The filtrate was subsequently extracted twice with equal volumes of ethyl acetate (Sigma-Aldrich). The organic extract was dried with sodium sulfate, filtered through a Whatman #1 filter paper, and brought to dryness using a rotary vacuum evaporator. Samples were reconstituted in 1 mL of 1:1 acetonitrile:water (Fisher Scientific) and filtered through a 0.45-μM polytetrafluoroethylene (PTFE) filter (Chromatographic Specialties Inc., ON, CA) into a 2-mL amber glass HPLC vial for LC–MS analysis.

### 2.4. LC–MS detection of iron-containing siderophores

All samples were analyzed by high-resolution LC–MS performed on a Q-Exactive Orbitrap mass spectrometer (Thermo Scientific, MA, USA) coupled to an Agilent 1290 HPLC system (CA, USA). Analytes were separated using an Eclipse Plus C18 RRHD column (2.1 × 100 mm, 1.8 μm; Agilent Technologies, CA, USA) maintained at 35°C. The mobile phase consisted of Optima grade (Fisher Scientific) water + 0.1% formic acid (*v/v*) (A) and acetonitrile + 0.1% formic acid (*v/v*) (B). The elution gradient was held at 0% B for 0.5 min, increased to 100% B over 3.5 min, held at 100% B for 2.5 min, and then returned to 0% B over 0.5 min. The sample injection volume and flow rate were 5 μL and 0.3 mL/min, respectively.

Analytes were ionized by heated electrospray ionization operating in the positive ionization mode with the following settings: capillary voltage, 3.9 kV; capillary temperature, 400 °C; sheath gas, 19 units; auxiliary gas, 8 units; probe heater temperature, 450°C; and S-Lens RF level, 45.00. Data were acquired using an untargeted data-dependent acquisition method. This consisted of a full MS scan at 140,000 resolution, with an *m/z* scan range of 106.7–1600, a automatic gain control target of $3 \times 10^6$, and a maximum injection time of 512 ms. The top two ions by intensity from each full scan were selected for MS/MS analysis using an *m/z* isolation window of 1.0. MS/MS parameters were as follows: resolution, 17,500; automatic gain control target, $1 \times 10^6$; maximum injection time, 65 ms; normalized collision energy, 35; intensity threshold, $1.5 \times 10^5$; and dynamic exclusion, 5 s.

For the detection of potential iron-containing compounds, a similar strategy to that used by Andersen et al [13] for detection of chlorine-, bromine-, and sulfur-containing metabolites was used. The raw LC–MS data files were imported into MZmine 2, and a peak list was generated using the chromatogram builder function with a minimum LC peak width of 0.2 min, an *m/z* tolerance of 5 ppm, and a minimum peak intensity of $1.0 \times 10^5$ [14]. Peak pairs within the peak list that had matching retention times (±0.02 min) and an *m/z* difference of 1.9953 Da (±3 ppm) were identified using the adduct search function in MZmine 2. These peak pairs represent putative iron-containing compounds as $^{54}Fe$ (natural abundance, 5.85%) occurs 1.9953 Da below the monoisotopic peak containing $^{56}Fe$ (natural abundance, 91.75%).

### 2.5. Isolation of the siderophore

The strain DAOMC 251601 was grown in bulk (5 L) and extracted as mentioned previously. The siderophore was isolated in a two-step fractionation process: a normal-phase separation followed

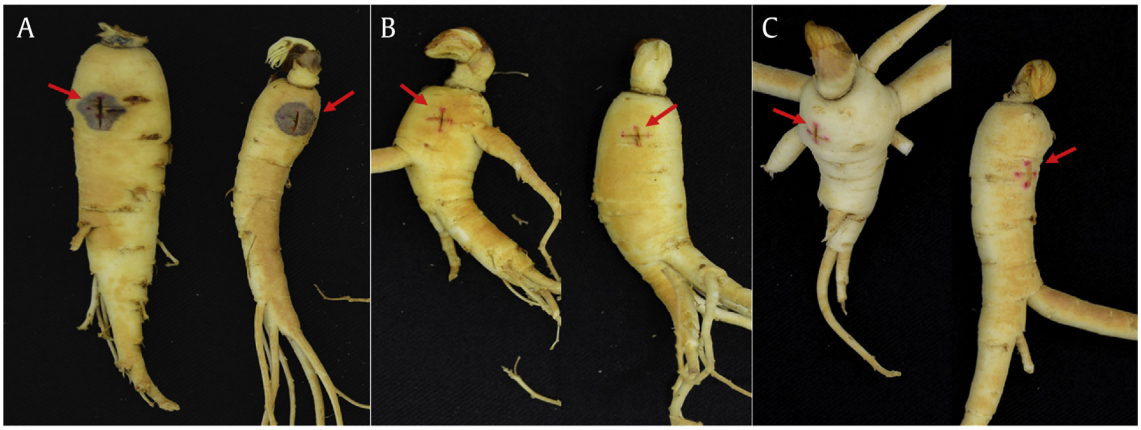


**Fig. 1. Ginseng roots infected with virulent and avirulent pathogenic fungi**. Comparison of root rot disease onset in American ginseng by *Ilyonectria* and *Cylindrocarpon* using (A) a virulent strain 251601, (B) an avirulent strain KAS 8150, and (C) control roots that were cut but not inoculated. Red arrows highlight the 5-mm cross-incision where the plugs were placed over and the disease lesion in the case of 251601 (A). Plugs were removed, and the exterior of the roots was washed before taking a photo. Nontargeted LC–MS detection of iron-containing compounds in extracts of *Ilyonectria* mors-panacis.

by a reverse-phase isolation. For the normal-phase procedure, the dried extract was reconstituted in 5 mL of methanol (Sigma-Aldrich) and mixed with 15 mL of chloroform (Sigma-Aldrich). The resuspended extract was separated using a Buchi Sepacore® flash system (Flawil, Switzerland) with normal-phase conditions. A 24-g RediSep® Rf (Lincoln, NE, USA) normal-phase silica column was used as a stationary phase, and the mobile phase consisted of chloroform (A) and methanol (B) (Sigma). A 20-min separation with a flow rate of 25 mL/min was used for the following method: the column was equilibrated to 100% A, the extract was injected, and A was held at 100% for 4 min. Solvent B was increased to 20% over 12 min and held there for 4 more min. A total of 12 fractions were collected throughout the entire method, collecting by volume. Fractions containing the putative siderophore by LC–MS screening were pooled together and dried. The pooled fractions were reconstituted in 1 mL of 50% methanol and purified by reverse-phase HPLC, performed on an Agilent 1200 system (CA, USA). An Eclipse XDB-C18 column (9.4 × 250 mm, 5 μm; Agilent Technologies) maintained at 35°C was used, with a mobile phase of HPLC-grade water + 0.1% trifluoroacetic acid (TFA) (*v*/*v*) (A) and acetonitrile + 0.1% TFA (*v*/*v*) (B) (HPLC-grade; Sigma-Aldrich). The injection volume and flow rate were 100 μL and 4 mL/min, respectively. The gradient was held at 15% B for 2 min, increased to 70% B over 13 min, increased to 100% B over 0.5 min, held at 100% B for 2 min, and then returned to 15% B over 0.5 min. The analytes were monitored and collected based on absorbance signals at 254 nm.

### 2.6. Siderophore production assays

Six strains (Table 1) were grown in quadruplicate in unaltered Potato Dextrose Broth (PDB) media. The natural iron concentration of the control medium was determined to be 1.01 ± 0.02 μM by ICP (Inductively Coupled Plasma)–MS analysis (Biotron facility, Western University, ON, CA). The strains were grown in 30 mL of PDB in 125-mL Erlenmeyer flasks capped with foam plugs and inoculated with 1 mL of the macerated fungal material, as previously described. The effect of iron concentration on siderophore production was also investigated by supplementing media with iron ($FeCl_3 \bullet 6\ H_2O$). Strains 251601 and 251609 were supplemented with 5 μM of $Fe^{3+}$ or 50 μM of $Fe^{3+}$ and grown in unaltered PDB. To monitor the effect of competing chelators in the environment, cultures of media were prepared by supplementing with EDTA • 2 $H_2O$ (Sigma-Aldrich) at concentrations of 5 μM and 50 μM. All samples were grown in quadruplicate. For all cultures, 100-μL aliquots of growth media were removed from the cultures every 4 days for 20 days and were then diluted in the ratio of 1:1 with methanol and stored at −20 °C. Immediately, before LC–MS analysis, the aliquots were supplemented with 100 μL of a 0.132-μM $FeCl_3 \bullet 6\ H_2O$ iron solution to shift siderophores to the chelated state.

## 3. Results

### 3.1. Disease virulence assessment

After three weeks of incubation at 21°C, the lesion diameter on the ginseng was measured. In agreement with previous work, DAOMC 251601, 251604, and 251605 were confirmed to be virulent, whereas 251608, 251609, and KAS8150 were confirmed to be avirulent (data shown in Table 2) [7]. Fig. 1 shows a comparison between 251601, KAS 8150, and healthy roots, highlighting the disease area.

The major peak detected with the iron isotope pattern had an *m*/*z* of 906.3304 and an isotopic profile that matches a formula $C_{39}H_{58}FeN_6O_{15}$ (Fig. 2). Screening of all fungal isolates revealed this to be the only iron-containing compound that was detected using this semitargeted strategy. The iron-chelated metabolite was only detected in strains that were identified as virulent (Table 2). In every extract where $C_{39}H_{58}FeN_6O_{15}$ was detected, an *m*/*z* of 853.4123 was also observed. The *m*/*z* difference between these ions is 52.9181 Da, indicating the bound and unbound form of the siderophore.

The chemical formula $C_{39}H_{58}FeN_6O_{15}$ was consistent with the known siderophore N,N′,N″-triacetylfusarinine C (TAFC) (Fig. 3)

**Table 2**
Lesion diameters virulence assays of *Ilyonectria* and *Cylindrocarpon* on 2-year-old American Ginseng.

| Strain (DOAMC) | Lesion diameter (mm) | Virulent/avirulent |
|---|---|---|
| 251601 | 10.5 ± 1.29 | Virulent |
| 251604 | 12.5 ± 1.29 | Virulent |
| 251605 | 11.0 ± 1.15 | Virulent |
| 251608 | 0 ± 0 | Avirulent |
| KAS8150 | 1.0 ± 0.82 | Avirulent |
| 251609 | 1.5 ± 1.29 | Avirulent |
| Control | 0 ± 0 | —— |

Lesions exceeding the incision diameter were considered virulent. DAOMC, Canadian Collection of Fungal Cultures.

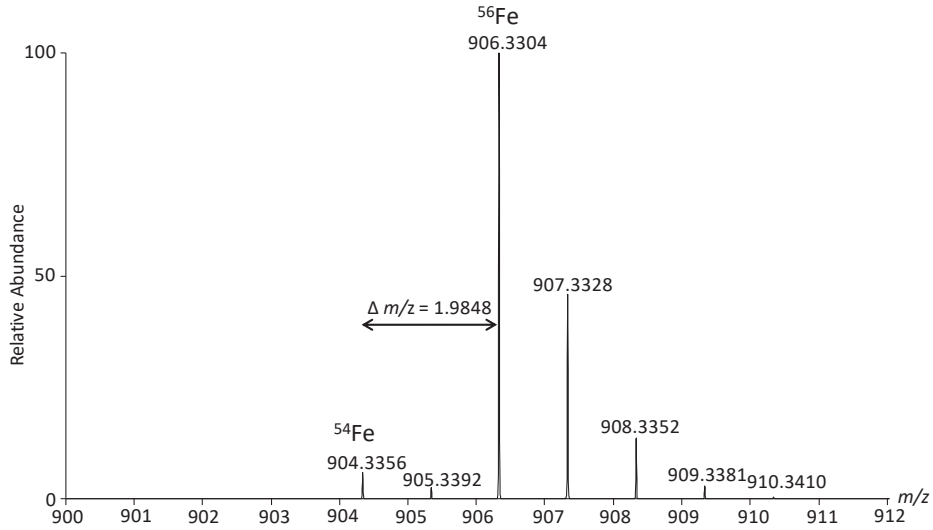


**Fig. 2. Positive-mode ESI isotope pattern of $[M+H]^+$ ion of $C_{39}H_{58}FeN_6O_{15}$.** This shows the unique isotope pattern indicating presence of $^{54}Fe$ in relation to $^{56}Fe$. Isolation and identification of N,N′,N″-triacetylfusarinine C as the predominant siderophore of *Ilyonectria*.
ESI, electrospray ionization.

[15]. Examination of the MS/MS fragmentation pattern of the nonchelated precursor ion at *m/z* 853.4123 (Fig. 4) revealed two neutral losses of 284.135 Da, leaving a product ion with an *m/z* of 285.1421. This product ion and neutral losses each correspond to the three *N*-acetylfusarinine ($C_{13}H_{20}N_2O_5$)—repeating units of TAFC [16]. The isolated compound was confirmed by $^1H$ NMR (supplementary figure S1) by comparison to previously acquired spectra of TAFC [17]. Purified TAFC + Fe was quantified by absorbance ($\varepsilon_{440}$ = 2960 $M^{-1}$ $cm^{-1}$) [16] and was used to prepare a standard curve for further quantification in subsequent assays.

### 3.2. TAFC production in virulent and avirulent strains

Samples were monitored over a period of 20 days as described in the Materials and methods section. The maximum production of TAFC occurred on Day 8 for all strains that produced TAFC (supplementary Figure S2). $Fe^{3+}$ was supplemented in samples before analysis, such that the concentration of $Fe^{3+}$ was five-fold higher than that of the unbound TAFC, to ensure TAFC was present in the chelated form for quantitation.

The virulent strains DAOMC 251601 and 251604 produced 7.53 and 8.73 mg/L of TAFC, respectively, whereas the avirulent strains DAOMC 251608, DAOMC 251609, and KAS8150 produced no detectable TAFC under these conditions (Fig. 5). Among the virulent strains, we found that DAOMC 251605, also a virulent isolate of *I. mors-panacis*, produced very little TAFC (0.09 mg/L) in comparison with other virulent strains.

### 3.3. Effect of iron concentration on production of TAFC

To determine the effect of $Fe^{3+}$ concentration on TAFC, DAOMC 251601 (virulent) and DAOMC 251609 (avirulent) were grown

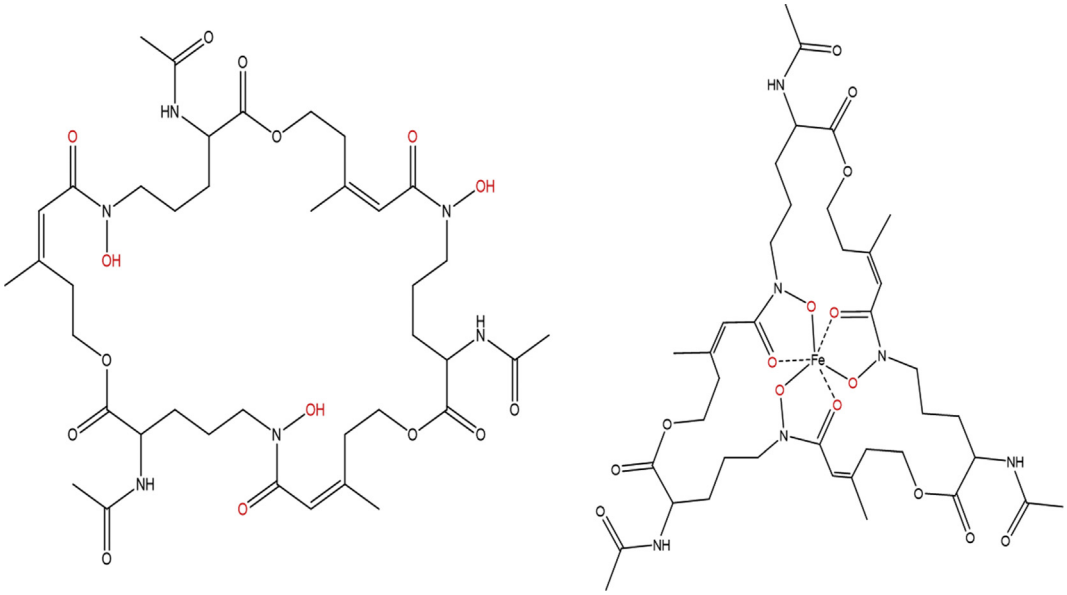


**Fig. 3. Molecular structure of N,N′,N″-triacetylfusarinine C**. Structures of N,N′,N″-triacetylfusarinine C in (left) unbound and (right) bound forms. Highlighted in red are the oxygen functional groups that are directly involved in chelating $Fe^{3+}$.

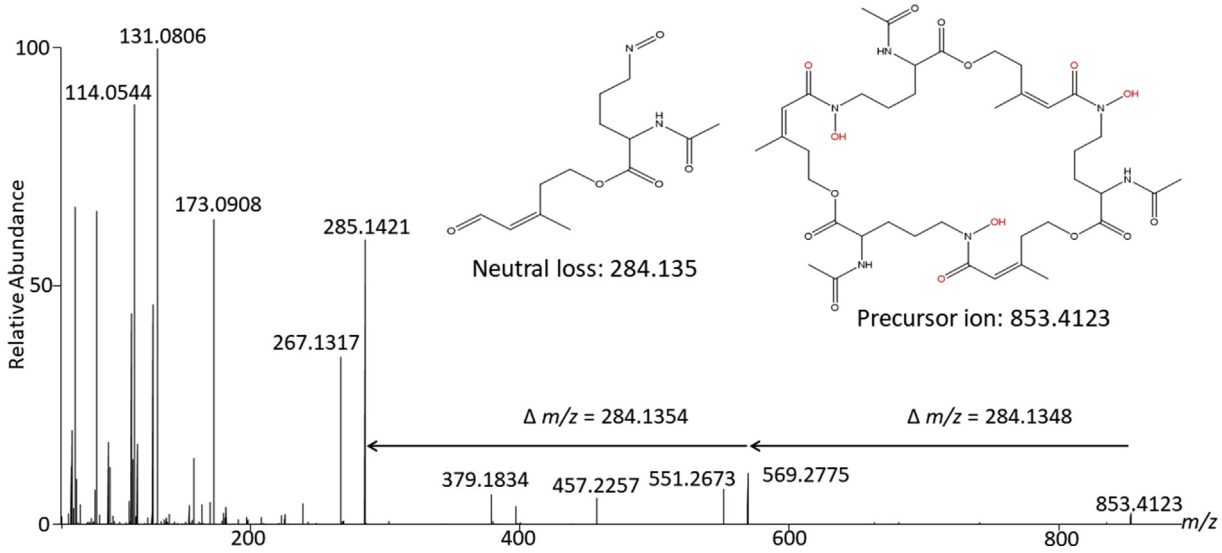


**Fig. 4. MS/MS of unbound N,N′,N″-triacetylfusarinine C**. Stepped 25/55 NCE MS/MS spectra of unbound N,N′,N″-triacetylfusarinine C. Diagnostic product ions of an *m/z* of 285.1421 and 569.2775. NCE, normalized collision energy.

under five different conditions: two supplemented concentrations of $Fe^{3+}$, two supplemented concentrations of EDTA, and control media. Comparing all conditions, only DAOMC 251601 produced detectable levels of TAFC, only when the growth media was not supplemented with $Fe^{3+}$ (Fig. 6). The addition of 5 μM of EDTA resulted in a decrease in the detection of iron-bound TAFC, while 50 μM of EDTA did not further decrease the amount detected.

## 4. Discussion

Siderophores are important metabolites in the development of fungi during iron-depleted conditions [10,18]. Siderophore production in *I. mors-panacis* has been observed, and it has been proposed to be related to virulence of root rot disease in American ginseng [9,10]. However, the siderophore was not chemically characterized. This is the first report of an identified siderophore in an *Ilyonectria* sp. Applying nontargeted LC–MS screening to the strains revealed no additional iron-containing compounds. This suggests that TAFC is the only or the most abundant siderophore synthesized by *I. mors-panacis*. Interestingly, no iron-containing compounds were found in the avirulent strains of *Ilyonectria* and *Cylindrocarpon* species, suggesting the avirulent strains favored other methods of iron encapsulation, perhaps membrane-bound ion channels [11,19].

Strains were compared for production of TAFC by monitoring the concentration of iron(III)-bound TAFC in extracellular media. Strains that were determined to be virulent by the lesion assay produced TAFC, whereas none was detected in extracts of avirulent strains. DAOMC 251605 produced less TAFC than the other virulent strains, although it was still present in all replicates. The reduced production of TAFC may be due to increased sensitivity of this strain to the presence of available iron, or the strain may naturally produce less TAFC. It is important to note that DAOMC 201601 turned off TAFC production at 5 μM of $FeCl_3$ and the background amount of iron in the unaltered PDB media is 1 μM, so decreased TAFC production in response to iron is observed in other virulent strains. This suggests that TAFC is a factor in disease virulence but not its sole contributor.

In addition, TAFC was the only iron chelator detected in our semitargeted screening for iron-containing compounds among all strains. Combined with previous research connecting siderophore production to virulent strains of fungi, the direct monitoring of siderophore concentration supports the suggestion that siderophores contribute to viability of *I. mors-panacis* in causing ginseng root rot disease. However, it is currently unknown if this metabolite directly contributes to the plant–pathogen interaction or if it is only used for growth *of I. mors-panacis*.

An important observation in the full MS spectra is the *m/z* difference of 18.0102 Da from the precursor ion for unbound TAFC. This *m/z* difference indicates a loss of $H_2O$. This is probably the consequence of the loss of a hydroxamate functional group, confirmed by peak shifts in the HNMR spectra. Moreover, this loss can be observed in up to three distinct steps, corresponding to the loss of all three hydroxamates. We observed that if hydroxamate functional groups are lost, TAFC is no longer capable of chelating iron. This agrees with similar reports that the loss of these

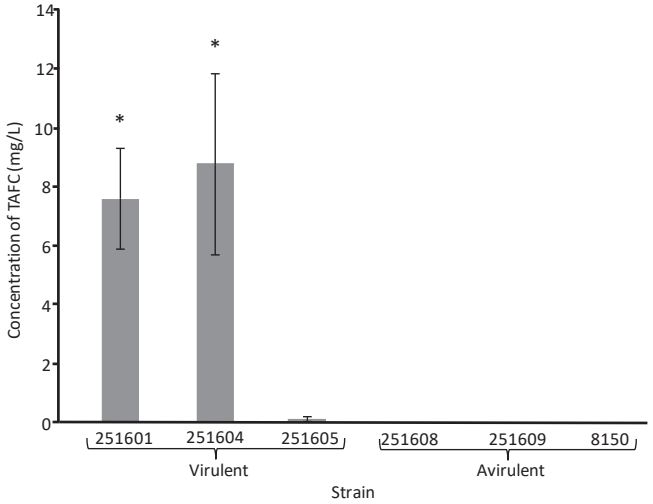


**Fig. 5. N,N′,N″-Triacetylfusarinine C production under unaltered PDB conditions**. Gray bars represent concentration of TAFC as an average. Error bars represent standard deviation across replicates (n = 3) in a sample. Grouping was performed by a pair-wise multiple comparison (Holm–Sidak method) where $p \leq 0.05$. Groups are denoted by the presence or absence of *. TAFC, N,N′,N″-triacetylfusarinine C. PDB, Potato Dextrose Broth.

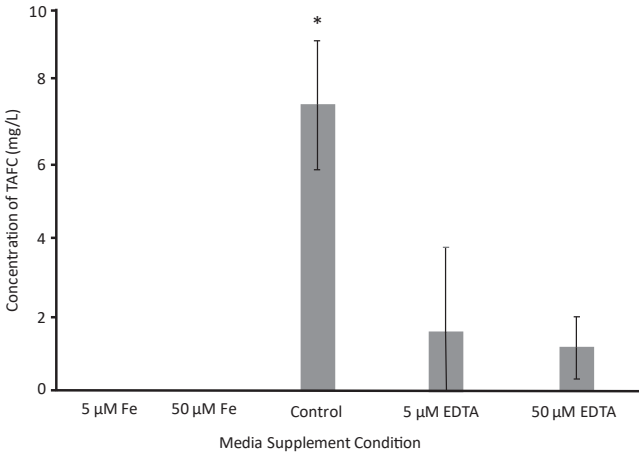


**Fig. 6. N,N′,N″-Triacetylfusarinine C concentration in media of strain DAOMC 251601 comparing concentrations of EDTA and iron in media**. Different concentrations of EDTA- and iron-supplemented media of strain DAOMC 251601 are displayed. Gray bars represent concentration of TAFC as an average. Error bars represent standard deviation across replicates (n = 3) in a sample. The control represents no alterations to PDB media. Grouping was performed by a pair-wise multiple comparison (Holm–Sidak method) where $p \leq 0.05$. Groups are denoted by the presence or absence of *. EDTA, ethylenediaminetetraacetic acid; TAFC, N,N′,N″-triacetylfusarinine C; PDB, Potato Dextrose Broth.

functional groups results in impaired TAFC function and could result in a significant decrease in fungal growth [19,20].

The concentration of iron in the environment is an important factor in root rot disease virulence. The previous literature has shown *Ilyonectria* spp. in American ginseng are more virulent when a greater concentration of iron is introduced into the environment [9,10]. Rahman and Punja [10] suggested this is a consequence of siderophore production, which was observed using a chrome azurol S medium growth assay. This is in contrast to the generally accepted theory that as the concentration of free iron increases in a medium, siderophore production is suppressed and the cell instead favors membrane-bound channels for iron uptake [12]. We created an assay with five different environmental conditions for iron availability. All samples that had iron supplemented showed no TAFC production, consistent with previous research [21]. When EDTA was added, it decreased the overall concentration of chelated TAFC. It is unclear whether this is because EDTA competes with TAFC for iron, or whether EDTA represses the production of the metabolite. Notably, it was found that regardless of concentration or availability of iron in the media, the nonvirulent strain DAOMC 251609 did not produce TAFC in detectable amounts. This further suggests that siderophores play an important role in root rot disease.

Previous reports from other fungal genera such as *Aspergillus* have demonstrated that siderophores are crucial to the growth of some fungi in low-iron conditions [11,19,20]. TAFC is a common siderophore for *Aspergillus fumigatus* and *Aspergillus nidulans*, and its production is related to the virulence of these fungi toward humans. Complete knockout of the biosynthetic pathway responsible for TAFC production resulted in no fungal growth in low-iron conditions [19]. As a result, it was suggested that siderophore production could be targeted to mediate disease in a very large range of systems, such as crop disease such as root rot and even in human fungal disease [20,22]. The development of a small-molecule inhibitor or other methods of control for TAFC production could be applied to limit the growth of *I. mors-panacis*, making it a candidate for root rot disease management that will be the focus of future studies.

## 5. Conclusion

Root rot affects 20–30% of ginseng crop yield in Canada annually. The cause of this disease is the soilborne fungus *I. mors-panacis*. The previous literature on this disease suggests several factors for increased virulence, most notably to this study are soil iron concentration and siderophore production. In this report, we identified the siderophore as TAFC, which was detected for the first time in an *Ilyonectria* sp. In addition, this was the only siderophore identified in the culture extracts, suggesting it is a key metabolite for fungal species that are virulent to ginseng. We compared the production of this metabolite across several strains of *Ilyonectria* and one strain of *Cylindrocarpon,* finding that virulent strains produced the siderophore whereas avirulent strains did not. We monitored the production of TAFC in different concentrations of supplemented iron and competing chelators. We found that TAFC is not produced when there is an excess of free iron in media, and EDTA decreases the amount of iron-bound TAFC in the media. Root rot remains an issue for ginseng farmers and causes a substantial loss of quality and yield for the industry. Siderophores are a known factor of root rot virulence, and until now, the specific siderophore was unidentified. The identification of this metabolite gives us further insights into and a greater understanding of the disease. Developing a method for the management of TAFC production by *Ilyonectria mors-panacis* could be an effective method for root rot management to be used by ginseng farmers, increasing crop yields and crop stability.

## Conflicts of interest

Authors declare no conflict of interest.

## Acknowledgments

The authors thank Dr Sean Westerveld for his collaboration with this publication, as well as Ontario Ministry of Agriculture, Food and Rural Affairs (OMAFRA) and the Ontario Ginseng Growers Association for their donation of ginseng. This project was supported by an Agriculture and Agri-Food Canada (AAFC) grant #3022 (M.W.S. and K.A.S.). Western University provided support to J.P.W. and N.D. through a teaching assistantship.

## Appendix A. Supplementary data

Supplementary data to this article can be found online at https://doi.org/10.1016/j.jgr.2019.08.008.

## References

[1] Lü J-M, Yao Q, Chen C. Ginseng compounds: an update on their molecular mechanisms and medical applications. Curr Vasc Pharmacol 2009;7(3):293–302. PubMed PMID: 19601854.
[2] Westerveld S. Ginseng production in ontario: ontario ministry of agriculture, food and rural affairs. 2010 [cited 2018 August 13]. Available from: http://www.omafra.gov.on.ca/english/crops/facts/10-081W.htm#seed.
[3] Baeg I-H, So S-H. The world ginseng market and the ginseng (Korea). J Ginseng Res 2013;37(1):1–7. https://doi.org/10.5142/jgr.2013.37.1. PubMed PMID: 23717152.
[4] Dong L, Xu J, Li Y, Fang H, Niu W, Li X, Zhang Y, Ding W, Chen S. Manipulation of microbial community in the rhizosphere alleviates the replanting issues in Panax ginseng. Soil Biol Biochem 2018;125:64–74. https://doi.org/10.1016/j.soilbio.2018.06.028.
[5] Howard RJ, Garland JA, Seaman WL. Diseases and pests of vegetable crops in Canada. Canadian Phytopathological Society; 1994.
[6] Cabral A, Groenewald JZ, Rego C, Oliveira H, Crous PW. Cylindrocarpon root rot: multi-gene analysis reveals novel species within the Ilyonectria radicicola species complex. Mycol Prog 2012;11(3):655–88. https://doi.org/10.1007/s11557-011-0777-7.
[7] Seifert KA, McMullen CR, Yee D, Reeleder RD, Dobinson KF. Molecular differentiation and detection of ginseng-adapted isolates of the root rot fungus

Cylindrocarpon destructans. Phytopathology 2003;93(12):1533–42. https://doi.org/10.1094/PHYTO.2003.93.12.1533.
[8] Farh ME-A, Kim Y-J, Kim Y-J, Yang D-C. Cylindrocarpon destructans/Ilyonectria radicicola-species complex: causative agent of ginseng root-rot disease and rusty symptoms. J Ginseng Res 2018;42(1):9–15. https://doi.org/10.1016/j.jgr.2017.01.004.
[9] Rahman M, Punja ZK. Factors influencing development of root rot on ginseng caused by Cylindrocarpon destructans. Phytopathology 2005;95(12):1381–90. https://doi.org/10.1094/PHYTO-95-1381.
[10] Rahman M, Punja ZK. Influence of iron on Cylindrocarpon root rot development on ginseng. Phytopathology 2006;96(11):1179–87. https://doi.org/10.1094/PHYTO-96-1179.
[11] Kragl C, Schrettl M, Abt B, Sarg B, Lindner HH, Haas H. EstB-mediated hydrolysis of the siderophore triacetylfusarinine C optimizes iron uptake of Aspergillus fumigatus. Eukaryotic Cell 2007;6(8):1278.
[12] Haas H. Molecular genetics of fungal siderophore biosynthesis and uptake: the role of siderophores in iron uptake and storage. Appl Microbiol Biotechnol 2003;62(4):316–30. https://doi.org/10.1007/s00253-003-1335-2.
[13] Andersen AJC, Hansen PJ, Jørgensen K, Nielsen KF. Dynamic cluster Analysis: an unbiased method for identifying a + 2 element containing compounds in liquid chromatographic high-resolution time-of-flight mass spectrometric data. Anal Chem 2016;88(24):12461–9. https://doi.org/10.1021/acs.analchem.6b03902.
[14] Pluskal T, Castillo S, Villar-Briones A, Orešič M. MZmine 2: modular framework for processing, visualizing, and analyzing mass spectrometry-based molecular profile data. BMC Bioinform 2010;11(1):395.
[15] Hossain MB, Eng-Wilmot DL, Loghry RA, Van der Helm D. Circular dichroism, crystal structure, and absolute configuration of the siderophore ferric N,N',N"-triacetylfusarinine, FeC39H57N6O15. J Am Chem Soc 1980;102(18):5766–73. https://doi.org/10.1021/ja00538a012.
[16] Emery T. A convenient assay for siderochrome hydrolytic enzymes. Anal Biochem 1976;71(1):294–9. https://doi.org/10.1016/0003-2697(76)90039-7.
[17] Diekmann H, Zähner H. Konstitution von Fusigen und dessen Abbau zu Δ2-Anhydromevalonsäurelacton. Eur J Biochem 1967;3(2):213–8.
[18] Carroll CS, Amankwa LN, Pinto LJ, Fuller JD, Moore MM. Detection of a serum siderophore by LC-MS/MS as a potential biomarker of invasive aspergillosis. PLoS One 2016;11(3):e0151260. https://doi.org/10.1371/journal.pone.0151260.
[19] Eisendle M, Oberegger H, Zadra I, Haas H. The siderophore system is essential for viability of Aspergillus nidulans: functional analysis of two genes encoding l-ornithine N 5-monooxygenase (sidA) and a non-ribosomal peptide synthetase (sidC). Mol Microbiol 2003;49(2):359–75. https://doi.org/10.1046/j.1365-2958.2003.03586.x.
[20] Frederick RE, Mayfield JA, DuBois JL. Iron trafficking as an antimicrobial target. BioMetals 2009;22(4):583. https://doi.org/10.1007/s10534-009-9236-1.
[21] Cabaj A, Kosakowska A. Iron-dependent growth of and siderophore production by two heterotrophic bacteria isolated from brackish water of the southern Baltic Sea. Microbiol Res 2009;164(5):570–7. https://doi.org/10.1016/j.micres.2007.07.001.
[22] Fekete FA, Chandhoke V, Jellison J. Iron-binding compounds produced by wood-decaying basidiomycetes. Appl Environ Microbiol 1989;55(10):2720–2. PubMed PMID: 16348038.